Production of Λ^{0}, Λ[over ¯]^{0}, Ξ^{±}, and Ω^{±} hyperons in pp[over ¯] collisions at sqrt[s]=1.96 TeV

T. Aaltonen *et al.* (CDF Collaboration)

Phys. Rev. D **86**, 012002 — Published 13 July 2012

DOI: 10.1103/PhysRevD.86.012002

Production of Λ^0, $\overline{\Lambda}^0$, $\Xi^\pm$, and $\Omega^\pm$ Hyperons in $p\overline{p}$ Collisions at $\sqrt{s} = 1.96$ TeV

T. Aaltonen,[22] B. Álvarez González[v],[10] S. Amerio,[42] D. Amidei,[33] A. Anastassov,[37] A. Annovi,[18] J. Antos,[13] G. Apollinari,[16] J.A. Appel,[16] A. Apresyan,[47] T. Arisawa,[56] A. Artikov,[14] J. Asaadi,[52] W. Ashmanskas,[16] B. Auerbach,[59] A. Aurisano,[52] F. Azfar,[41] W. Badgett,[16] A. Barbaro-Galtieri,[27] V.E. Barnes,[47] B.A. Barnett,[24] P. Barria[ee],[45] P. Bartos,[13] M. Bauce[cc],[42] G. Bauer,[31] F. Bedeschi,[45] D. Beecher,[29] S. Behari,[24] G. Bellettini[dd],[45] J. Bellinger,[58] D. Benjamin,[15] A. Beretvas,[16] A. Bhatti,[49] M. Binkley[*],[16] D. Bisello[cc],[42] I. Bizjak[ii],[29] K.R. Bland,[5] C. Blocker,[7] B. Blumenfeld,[24] A. Bocci,[15] A. Bodek,[48] D. Bortoletto,[47] J. Boudreau,[46] A. Boveia,[12] B. Brau[a],[16] L. Brigliadori[bb],[6] A. Brisuda,[13] C. Bromberg,[34] E. Brucken,[22] M. Bucciantonio[dd],[45] J. Budagov,[14] H.S. Budd,[48] S. Budd,[23] K. Burkett,[16] G. Busetto[cc],[42] P. Bussey,[20] A. Buzatu,[32] S. Cabrera[x],[15] C. Calancha,[30] S. Camarda,[4] M. Campanelli,[34] M. Campbell,[33] F. Canelli[12],[16] A. Canepa,[44] B. Carls,[23] D. Carlsmith,[58] R. Carosi,[45] S. Carrillo[k],[17] S. Carron,[16] B. Casal,[10] M. Casarsa,[16] A. Castro[bb],[6] P. Catastini,[16] D. Cauz,[53] V. Cavaliere[ee],[45] M. Cavalli-Sforza,[4] A. Cerri[f],[27] L. Cerrito[q],[29] Y.C. Chen,[1] M. Chertok,[8] G. Chiarelli,[45] G. Chlachidze,[16] F. Chlebana,[16] K. Cho,[26] D. Chokheli,[14] J.P. Chou,[21] W.H. Chung,[58] Y.S. Chung,[48] C.I. Ciobanu,[43] M.A. Ciocci[ee],[45] A. Clark,[19] D. Clark,[7] G. Compostella[cc],[42] M.E. Convery,[16] J. Conway,[8] M.Corbo,[43] M. Cordelli,[18] C.A. Cox,[8] D.J. Cox,[8] F. Crescioli[dd],[45] C. Cuenca Almenar,[59] J. Cuevas[v],[10] R. Culbertson,[16] D. Dagenhart,[16] N. d'Ascenzo[t],[43] M. Datta,[16] P. de Barbaro,[48] S. De Cecco,[50] G. De Lorenzo,[4] M. Dell'Orso[dd],[45] C. Deluca,[4] L. Demortier,[49] J. Deng[c],[15] M. Deninno,[6] F. Devoto,[22] M. d'Errico[cc],[42] A. Di Canto[dd],[45] B. Di Ruzza,[45] J.R. Dittmann,[5] M. D'Onofrio,[28] S. Donati[dd],[45] P. Dong,[16] T. Dorigo,[42] K. Ebina,[56] A. Elagin,[52] A. Eppig,[33] R. Erbacher,[8] D. Errede,[23] S. Errede,[23] N. Ershaidat[aa],[43] R. Eusebi,[52] H.C. Fang,[27] S. Farrington,[41] M. Feindt,[25] J.P. Fernandez,[30] C. Ferrazza[ff],[45] R. Field,[17] G. Flanagan[r],[47] R. Forrest,[8] M.J. Frank,[5] M. Franklin,[21] J.C. Freeman,[16] I. Furic,[17] M. Gallinaro,[49] J. Galyardt,[11] J.E. Garcia,[19] A.F. Garfinkel,[47] P. Garosi[ee],[45] H. Gerberich,[23] E. Gerchtein,[16] S. Giagu[gg],[50] V. Giakoumopoulou,[3] P. Giannetti,[45] K. Gibson,[46] C.M. Ginsburg,[16] N. Giokaris,[3] P. Giromini,[18] M. Giunta,[45] G. Giurgiu,[24] V. Glagolev,[14] D. Glenzinski,[16] M. Gold,[36] D. Goldin,[52] N. Goldschmidt,[17] A. Golossanov,[16] G. Gomez,[10] G. Gomez-Ceballos,[31] M. Goncharov,[31] O. González,[30] I. Gorelov,[36] A.T. Goshaw,[15] K. Goulianos,[49] A. Gresele,[42] S. Grinstein,[4] C. Grosso-Pilcher,[12] R.C. Group,[16] J. Guimaraes da Costa,[21] Z. Gunay-Unalan,[34] C. Haber,[27] S.R. Hahn,[16] E. Halkiadakis,[51] A. Hamaguchi,[40] J.Y. Han,[48] F. Happacher,[18] K. Hara,[54] D. Hare,[51] M. Hare,[55] R.F. Harr,[57] K. Hatakeyama,[5] C. Hays,[41] M. Heck,[25] J. Heinrich,[44] M. Herndon,[58] S. Hewamanage,[5] D. Hidas,[51] A. Hocker,[16] W. Hopkins[g],[16] D. Horn,[25] S. Hou,[1] R.E. Hughes,[38] M. Hurwitz,[12] U. Husemann,[59] N. Hussain,[32] M. Hussein,[34] J. Huston,[34] G. Introzzi,[45] M. Iori[gg],[50] A. Ivanov[o],[8] E. James,[16] D. Jang,[11] B. Jayatilaka,[15] E.J. Jeon,[26] M.K. Jha,[6] S. Jindariani,[16] W. Johnson,[8] M. Jones,[47] K.K. Joo,[26] S.Y. Jun,[11] T.R. Junk,[16] T. Kamon,[52] P.E. Karchin,[57] Y. Kato[n],[40] W. Ketchum,[12] J. Keung,[44] V. Khotilovich,[52] B. Kilminster,[16] D.H. Kim,[26] H.S. Kim,[26] H.W. Kim,[26] J.E. Kim,[26] M.J. Kim,[18] S.B. Kim,[26] S.H. Kim,[54] Y.K. Kim,[12] N. Kimura,[56] S. Klimenko,[17] K. Kondo,[56] D.J. Kong,[26] J. Konigsberg,[17] A. Korytov,[17] A.V. Kotwal,[15] M. Kreps,[25] J. Kroll,[44] D. Krop,[12] N. Krumnack[l],[5] M. Kruse,[15] V. Krutelyov[d],[52] T. Kuhr,[25] M. Kurata,[54] S. Kwang,[12] A.T. Laasanen,[47] S. Lami,[45] S. Lammel,[16] M. Lancaster,[29] R.L. Lander,[8] K. Lannon[u],[38] A. Lath,[51] G. Latino[ee],[45] I. Lazzizzera,[42] T. LeCompte,[2] E. Lee,[52] H.S. Lee,[12] J.S. Lee,[26] S.W. Lee[w],[52] S. Leo[dd],[45] S. Leone,[45] J.D. Lewis,[16] C.-J. Lin,[27] J. Linacre,[41] M. Lindgren,[16] E. Lipeles,[44] A. Lister,[19] D.O. Litvintsev,[16] C. Liu,[46] Q. Liu,[47] T. Liu,[16] S. Lockwitz,[59] N.S. Lockyer,[44] A. Loginov,[59] D. Lucchesi[cc],[42] J. Lueck,[25] P. Lujan,[27] P. Lukens,[16] G. Lungu,[49] J. Lys,[27] R. Lysak,[13] R. Madrak,[16] K. Maeshima,[16] K. Makhoul,[31] P. Maksimovic,[24] S. Malik,[49] G. Manca[b],[28] A. Manousakis-Katsikakis,[3] F. Margaroli,[47] C. Marino,[25] M. Martínez,[4] R. Martínez-Ballarín,[30] P. Mastrandrea,[50] M. Mathis,[24] M.E. Mattson,[57] P. Mazzanti,[6] K.S. McFarland,[48] P. McIntyre,[52] R. McNulty[i],[28] A. Mehta,[28] P. Mehtala,[22] A. Menzione,[45] C. Mesropian,[49] T. Miao,[16] D. Mietlicki,[33] A. Mitra,[1] H. Miyake,[54] S. Moed,[21] N. Moggi,[6] M.N. Mondragon[k],[16] C.S. Moon,[26] R. Moore,[16] M.J. Morello,[16] J. Morlock,[25] P. Movilla Fernandez,[16] A. Mukherjee,[16] Th. Muller,[25] P. Murat,[16] M. Mussini[bb],[6] J. Nachtman[m],[16] Y. Nagai,[54] J. Naganoma,[56] I. Nakano,[39] A. Napier,[55] J. Nett,[58] C. Neu[z],[44] M.S. Neubauer,[23] J. Nielsen[e],[27] L. Nodulman,[2] O. Norniella,[23] E. Nurse,[29] L. Oakes,[41] S.H. Oh,[15] Y.D. Oh,[26] I. Oksuzian,[17] T. Okusawa,[40] R. Orava,[22] L. Ortolan,[4] S. Pagan Griso[cc],[42] C. Pagliarone,[53] E. Palencia[f],[10] V. Papadimitriou,[16] A.A. Paramonov,[2] J. Patrick,[16] G. Pauletta[hh],[53] M. Paulini,[11] C. Paus,[31] D.E. Pellett,[8] A. Penzo,[53] T.J. Phillips,[15] G. Piacentino,[45] E. Pianori,[44] J. Pilot,[38] K. Pitts,[23] C. Plager,[9] L. Pondrom,[58] K. Potamianos,[47] O. Poukhov[*],[14] F. Prokoshin[y],[14] A. Pronko,[16] F. Ptohos[h],[18] E. Pueschel,[11] G. Punzi[dd],[45] J. Pursley,[58] A. Rahaman,[46] V. Ramakrishnan,[58] N. Ranjan,[47] I. Redondo,[30] P. Renton,[41] M. Rescigno,[50] F. Rimondi[bb],[6] L. Ristori[45],[16] A. Robson,[20] T. Rodrigo,[10] T. Rodriguez,[44] E. Rogers,[23] S. Rolli,[55] R. Roser,[16]

M. Rossi,[53] F. Ruffini[ee],[45] A. Ruiz,[10] J. Russ,[11] V. Rusu,[16] A. Safonov,[52] W.K. Sakumoto,[48] L. Santi[hh],[53] L. Sartori,[45] K. Sato,[54] V. Saveliev[t],[43] A. Savoy-Navarro,[43] P. Schlabach,[16] A. Schmidt,[25] E.E. Schmidt,[16] M.P. Schmidt[*],[59] M. Schmitt,[37] T. Schwarz,[8] L. Scodellaro,[10] A. Scribano[ee],[45] F. Scuri,[45] A. Sedov,[47] S. Seidel,[36] Y. Seiya,[40] A. Semenov,[14] F. Sforza[dd],[45] A. Sfyrla,[23] S.Z. Shalhout,[8] T. Shears,[28] P.F. Shepard,[46] M. Shimojima[s],[54] S. Shiraishi,[12] M. Shochet,[12] I. Shreyber,[35] A. Simonenko,[14] P. Sinervo,[32] A. Sissakian[*],[14] K. Sliwa,[55] J.R. Smith,[8] F.D. Snider,[16] A. Soha,[16] S. Somalwar,[51] V. Sorin,[4] P. Squillacioti,[16] M. Stanitzki,[59] R. St. Denis,[20] B. Stelzer,[32] O. Stelzer-Chilton,[32] D. Stentz,[37] J. Strologas,[36] G.L. Strycker,[33] Y. Sudo,[54] A. Sukhanov,[17] I. Suslov,[14] K. Takemasa,[54] Y. Takeuchi,[54] J. Tang,[12] M. Tecchio,[33] P.K. Teng,[1] J. Thom[g],[16] J. Thome,[11] G.A. Thompson,[23] E. Thomson,[44] P. Ttito-Guzmán,[30] S. Tkaczyk,[16] D. Toback,[52] S. Tokar,[13] K. Tollefson,[34] T. Tomura,[54] D. Tonelli,[16] S. Torre,[18] D. Torretta,[16] P. Totaro[hh],[53] M. Trovato[ff],[45] Y. Tu,[44] N. Turini[ee],[45] F. Ukegawa,[54] S. Uozumi,[26] A. Varganov,[33] E. Vataga[ff],[45] F. Vázquez[k],[17] G. Velev,[16] C. Vellidis,[3] M. Vidal,[30] I. Vila,[10] R. Vilar,[10] M. Vogel,[36] G. Volpi[dd],[45] P. Wagner,[44] R.L. Wagner,[16] T. Wakisaka,[40] R. Wallny,[9] C. Wang,[15] S.M. Wang,[1] A. Warburton,[32] D. Waters,[29] M. Weinberger,[52] A. Wen,[15] W.C. Wester III,[16] B. Whitehouse,[55] D. Whiteson[c],[44] A.B. Wicklund,[2] E. Wicklund,[16] S. Wilbur,[12] F. Wick,[25] H.H. Williams,[44] J.S. Wilson,[38] P. Wilson,[16] B.L. Winer,[38] P. Wittich[g],[16] S. Wolbers,[16] H. Wolfe,[38] T. Wright,[33] X. Wu,[19] Z. Wu,[5] K. Yamamoto,[40] J. Yamaoka,[15] U.K. Yang[p],[12] Y.C. Yang,[26] W.-M. Yao,[27] G.P. Yeh,[16] K. Yi[m],[16] J. Yoh,[16] K. Yorita,[56] T. Yoshida[j],[40] G.B. Yu,[15] I. Yu,[26] S.S. Yu,[16] J.C. Yun,[16] A. Zanetti,[53] Y. Zeng,[15] and S. Zucchelli[bb6]

(CDF Collaboration[†])

[1]Institute of Physics, Academia Sinica, Taipei, Taiwan 11529, Republic of China
[2]Argonne National Laboratory, Argonne, Illinois 60439, USA
[3]University of Athens, 157 71 Athens, Greece
[4]Institut de Fisica d'Altes Energies, Universitat Autonoma de Barcelona, E-08193, Bellaterra (Barcelona), Spain
[5]Baylor University, Waco, Texas 76798, USA
[6]Istituto Nazionale di Fisica Nucleare Bologna, [bb]University of Bologna, I-40127 Bologna, Italy
[7]Brandeis University, Waltham, Massachusetts 02254, USA
[8]University of California, Davis, Davis, California 95616, USA
[9]University of California, Los Angeles, Los Angeles, California 90024, USA
[10]Instituto de Fisica de Cantabria, CSIC-University of Cantabria, 39005 Santander, Spain
[11]Carnegie Mellon University, Pittsburgh, Pennsylvania 15213, USA
[12]Enrico Fermi Institute, University of Chicago, Chicago, Illinois 60637, USA
[13]Comenius University, 842 48 Bratislava, Slovakia; Institute of Experimental Physics, 040 01 Kosice, Slovakia
[14]Joint Institute for Nuclear Research, RU-141980 Dubna, Russia
[15]Duke University, Durham, North Carolina 27708, USA
[16]Fermi National Accelerator Laboratory, Batavia, Illinois 60510, USA
[17]University of Florida, Gainesville, Florida 32611, USA
[18]Laboratori Nazionali di Frascati, Istituto Nazionale di Fisica Nucleare, I-00044 Frascati, Italy
[19]University of Geneva, CH-1211 Geneva 4, Switzerland
[20]Glasgow University, Glasgow G12 8QQ, United Kingdom
[21]Harvard University, Cambridge, Massachusetts 02138, USA
[22]Division of High Energy Physics, Department of Physics, University of Helsinki and Helsinki Institute of Physics, FIN-00014, Helsinki, Finland
[23]University of Illinois, Urbana, Illinois 61801, USA
[24]The Johns Hopkins University, Baltimore, Maryland 21218, USA
[25]Institut für Experimentelle Kernphysik, Karlsruhe Institute of Technology, D-76131 Karlsruhe, Germany
[26]Center for High Energy Physics: Kyungpook National University, Daegu 702-701, Korea; Seoul National University, Seoul 151-742, Korea; Sungkyunkwan University, Suwon 440-746, Korea; Korea Institute of Science and Technology Information, Daejeon 305-806, Korea; Chonnam National University, Gwangju 500-757, Korea; Chonbuk National University, Jeonju 561-756, Korea
[27]Ernest Orlando Lawrence Berkeley National Laboratory, Berkeley, California 94720, USA
[28]University of Liverpool, Liverpool L69 7ZE, United Kingdom
[29]University College London, London WC1E 6BT, United Kingdom
[30]Centro de Investigaciones Energeticas Medioambientales y Tecnologicas, E-28040 Madrid, Spain
[31]Massachusetts Institute of Technology, Cambridge, Massachusetts 02139, USA
[32]Institute of Particle Physics: McGill University, Montréal, Québec, Canada H3A 2T8; Simon Fraser University, Burnaby, British Columbia, Canada V5A 1S6; University of Toronto, Toronto, Ontario, Canada M5S 1A7; and TRIUMF, Vancouver, British Columbia, Canada V6T 2A3
[33]University of Michigan, Ann Arbor, Michigan 48109, USA

[34]Michigan State University, East Lansing, Michigan 48824, USA
[35]Institution for Theoretical and Experimental Physics, ITEP, Moscow 117259, Russia
[36]University of New Mexico, Albuquerque, New Mexico 87131, USA
[37]Northwestern University, Evanston, Illinois 60208, USA
[38]The Ohio State University, Columbus, Ohio 43210, USA
[39]Okayama University, Okayama 700-8530, Japan
[40]Osaka City University, Osaka 588, Japan
[41]University of Oxford, Oxford OX1 3RH, United Kingdom
[42]Istituto Nazionale di Fisica Nucleare, Sezione di Padova-Trento, [cc]University of Padova, I-35131 Padova, Italy
[43]LPNHE, Universite Pierre et Marie Curie/IN2P3-CNRS, UMR7585, Paris, F-75252 France
[44]University of Pennsylvania, Philadelphia, Pennsylvania 19104, USA
[45]Istituto Nazionale di Fisica Nucleare Pisa, [dd]University of Pisa,
[ee]University of Siena and [ff]Scuola Normale Superiore, I-56127 Pisa, Italy
[46]University of Pittsburgh, Pittsburgh, Pennsylvania 15260, USA
[47]Purdue University, West Lafayette, Indiana 47907, USA
[48]University of Rochester, Rochester, New York 14627, USA
[49]The Rockefeller University, New York, New York 10065, USA
[50]Istituto Nazionale di Fisica Nucleare, Sezione di Roma 1,
[gg]Sapienza Università di Roma, I-00185 Roma, Italy
[51]Rutgers University, Piscataway, New Jersey 08855, USA
[52]Texas A&M University, College Station, Texas 77843, USA
[53]Istituto Nazionale di Fisica Nucleare Trieste/Udine,
I-34100 Trieste, [hh]University of Trieste/Udine, I-33100 Udine, Italy
[54]University of Tsukuba, Tsukuba, Ibaraki 305, Japan
[55]Tufts University, Medford, Massachusetts 02155, USA
[56]Waseda University, Tokyo 169, Japan
[57]Wayne State University, Detroit, Michigan 48201, USA
[58]University of Wisconsin, Madison, Wisconsin 53706, USA
[59]Yale University, New Haven, Connecticut 06520, USA

(Dated: June 22, 2012)

We report a set of measurements of inclusive invariant p_T differential cross sections of Λ^0, $\overline{\Lambda}^0$, $\Xi^\pm$, and $\Omega^\pm$ hyperons reconstructed in the central region with pseudorapidity $|\eta| < 1$ and p_T up to 10 GeV/c. Events are collected with a minimum-bias trigger in $p\bar{p}$ collisions at a center-of-mass energy of 1.96 TeV using the CDF II detector at the Tevatron Collider. As p_T increases, the slopes of the differential cross sections of the three particles are similar, which could indicate a universality of the particle production in p_T. The invariant differential cross sections are also presented for different charged-particle multiplicity intervals.

PACS numbers: 14.70.Pw, 13.85.Rm, 13.85.Qk, 14.80.-j

I. INTRODUCTION

Ever since their discovery in cosmic ray interactions [1], particles containing strange quarks have been extensively studied at particle colliders (e^+e^- [2], ep [3], $p\bar{p}$ [4, 5] and pp [6]). The process by which hadrons in general are produced from interactions is an unsolved problem in the standard model, and a detailed analysis of production properties of particles with different quark flavors and numbers of quarks could pave the way to understanding the process from first principles. The data on strange particle production can also be used to refine phenomenological models and set parameters, such as the strange quark suppression constant in event generators, which have become an integral part of any data analysis. Interest in particles containing strange quarks increased with the introduction of the quark-gluon plasma (QGP). Formation of quark-gluon plasma in a collision could manifest itself as an enhanced production of strange particles such as kaons and hyperons [7]. To isolate QGP sig-

*Deceased
†With visitors from [a]University of Massachusetts Amherst, Amherst, Massachusetts 01003, [b]Istituto Nazionale di Fisica Nucleare, Sezione di Cagliari, 09042 Monserrato (Cagliari), Italy, [c]University of California Irvine, Irvine, CA 92697, [d]University of California Santa Barbara, Santa Barbara, CA 93106 [e]University of California Santa Cruz, Santa Cruz, CA 95064, [f]CERN,CH-1211 Geneva, Switzerland, [g]Cornell University, Ithaca, NY 14853, [h]University of Cyprus, Nicosia CY-1678, Cyprus, [i]University College Dublin, Dublin 4, Ireland, [j]University of Fukui, Fukui City, Fukui Prefecture, Japan 910-0017, [k]Universidad Iberoamericana, Mexico D.F., Mexico, [l]Iowa State University, Ames, IA 50011, [m]University of Iowa, Iowa City, IA 52242, [n]Kinki University, Higashi-Osaka City, Japan 577-8502, [o]Kansas State University, Manhattan, KS 66506, [p]University of Manchester, Manchester M13 9PL, England, [q]Queen Mary, University of London, London, E1 4NS, England, [r]Muons, Inc., Batavia, IL 60510, [s]Nagasaki Institute of Applied Science, Nagasaki, Japan, [t]National Research Nuclear University, Moscow, Russia, [u]University of Notre Dame, Notre Dame, IN 46556, [v]Universidad de Oviedo, E-33007 Oviedo, Spain, [w]Texas Tech University, Lubbock, TX 79609, [x]IFIC(CSIC-Universitat de Valencia), 56071 Valencia, Spain, [y]Universidad Tecnica Federico Santa Maria, 110v Valparaiso, Chile, [z]University of Virginia, Charlottesville, VA 22906, [aa]Yarmouk University, Irbid 211-63, Jordan, [ii]On leave from J. Stefan Institute, Ljubljana, Slovenia,

natures in heavy-ion collision data, understanding the particle production properties from simple nucleon interactions is necessary.

There are ample data on the production of particles with one strange quark, but very little available on particles with two or more [8, 9]. Previous studies of hyperons from colliders such as RHIC [6], $Sp\overline{p}S$ [10], and the Tevatron [5, 11, 12] were limited by low sample statistics and the limited accessible range of hyperon momentum component transverse to the beam direction (p_T). In this analysis, we report on a study of the hyperons Λ^0 (quark content uds), Ξ^- (dss), and Ω^- (sss) and their corresponding antiparticles ($\overline{\Lambda}^0$, Ξ^+, and Ω^+). For these hyperons, the inclusive invariant p_T differential cross sections are measured up to p_T of 10 GeV/c, based on ~ 100 million minimum-bias events collected with the CDF II detector. The measurements reported here for $\Xi^\pm$ and $\Omega^\pm$ are the current best from any hadron collider experiment in terms of statistics and p_T range.

II. EVENT SELECTION

The CDF II detector is described in detail elsewhere [13]. The components most relevant to this analysis are those that comprise the tracking system, which is within a uniform axial magnetic field of 1.4T. The inner tracking volume is composed of a system of eight layers of silicon microstrip detectors ranging in radius from 1.5 to 28.0 cm [14] in the pseudorapidity region $|\eta| < 2$ [15]. The remainder of the tracking volume is occupied by the Central Outer Tracker (COT). The COT is a cylindrical drift chamber containing 96 sense-wire layers grouped in eight alternating superlayers of axial and stereo wires [16]. Its active volume covers 40 to 140 cm in radius and $|z| < 155$ cm. The transverse-momentum resolution of tracks reconstructed using COT hits is $\sigma(p_T)/p_T^2 \sim 0.0017/(\text{GeV}/c)$.

Events for this analysis are collected with a "minimum-bias" (MB) trigger, which selects beam crossings with at least one $p\bar{p}$ interaction by requiring a timing coincidence for signals in both forward and backward gas Cherenkov counters [17] covering the regions $3.7 < |\eta| < 4.7$. The MB trigger is rate-limited to keep the final trigger output at 1 Hz. Primary event vertices are identified by the convergence of reconstructed tracks along the beam axis. Events are accepted that contain a reconstructed vertex in the fiducial region $|z_{vtx}| \leq 60$ cm centered around the nominal CDF origin ($z = 0$). When an event has more than one vertex, the highest quality vertex, usually the one with the most associated tracks, is selected and it is required that there be no other vertices within ± 5 cm of this vertex. This selection introduces a bias toward high multiplicity events as the instantaneous luminosity increases. To combine events collected at different average instantaneous luminosities, we determine a per-event weight as a function of the charged-track multiplicity N_{ch} in order to match the multiplicity distribution of a data sample where the average number of interactions is less than 0.3 per bunch crossing. For the N_{ch} calculation, tracks are required to have a high track-fit quality with χ^2 per degree-of-freedom (χ^2/dof) less than 2.5, and more than five hits in at least two axial and two stereo COT segments. It is further required that tracks satisfy $|\eta| < 1$, impact parameter d_0 less than 0.25 cm, the distance along the z-axis (δZ_0) between the event vertex and the track position at the point of closest approach to the vertex in the $r-\phi$ plane be less than 2 cm, and $p_T > 0.3$ GeV/c. The p_T selection is to minimize the inefficiency of the track-finding algorithm for low momentum tracks.

III. RESONANCE RECONSTRUCTION

We search for $\Lambda^0 \to p\pi^-$ decays using tracks with opposite-sign charge and $p_T > 0.325$ GeV/c that satisfy the χ^2/dof and COT segment requirements. In this paper, any reference to a specific hyperon state implies the antiparticle state as well. For each two-track combination we calculate their intersection coordinate in the $r-\phi$ plane. Once this intersection point, referred to as the secondary vertex, is found, the z-coordinate of each track (Z_1 and Z_2) is calculated at that point. If the distance $|Z_1 - Z_2|$ is less than 1.5 cm, the tracks are considered to originate from a Λ^0 candidate decay. The pair is traced back to the vertex and we require δZ_0 be less than 2 cm, and the d_0 be less than 0.25 cm. To reduce backgrounds further, we require the Λ^0 decay length L_{Λ^0}, the distance in the $r-\phi$ plane between the primary and secondary vertices, to be greater than 2.5 cm and less than 50 cm.

The invariant mass $M_{p\pi}$ of the two-track system is calculated by attributing the proton mass to the track with the higher p_T, as preferentially expected by the kinematics of a Λ^0 decay. Figure 1 shows the invariant mass for Λ^0 candidates with $|\eta| < 1$. This distribution is divided into 23 p_T intervals [18] and the number of Λ^0 in each p_T interval is determined by fitting the invariant mass distributions using a Gaussian function with three parameters for the signal and a third-order polynomial for the underlying combinatorial background. The data in the mass range $1.10 - 1.16$ GeV/c^2 are fitted. The polynomial fit to the background is subtracted bin-by-bin from the data entries in the Λ^0 mass window ($1.111 - 1.121$ GeV/c^2) to obtain the number of Λ^0 hyperons. This number is divided by the acceptance to obtain the invariant differential p_T distribution as described later. With our minimum track p_T requirement, the Λ^0 p_T resolution decreases from $\sim$0.8% at 1.5 GeV/c to $\sim$0.6% at 3 GeV/c and slowly increases to $\sim$1.1% at 10 GeV/c.

The fitting procedure is one source of systematic uncertainty. This uncertainty is estimated by separately varying the mass range of the fit, the functional form for the signal to a double Gaussian, and the background modeling function to a second-order polynomial. The number of Λ^0 is recalculated in all p_T intervals for each variation. The systematic uncertainty is determined as the sum in quadrature of the fractional change in the number of Λ^0 from each modified fit. It decreases from $\pm 10\%$ at the lowest p_T (1.2 GeV/c) to less than $\pm 5\%$ for $p_T > 1.75$ GeV/c.

The cascade reconstruction decay mode is $\Xi^- \rightarrow \Lambda^0\pi^- \rightarrow (p\pi^-)\pi^-$. The previously reconstructed Λ^0 candidates are used, but without the d_0 and δZ_0 requirements. We select Λ^0 candidates in the Λ^0 mass window and calculate the coordinate of the intersection point in the $r-\phi$ plane between the Λ^0 candidate and a third track. The z-axis coordinates at this point are calculated for the third track (Z_3) and the Λ^0 candidate (Z_4). The three-track system is considered a Ξ^- candidate decay if the distance $|Z_3 - Z_4| < 1.5$ cm. We also require $L_{\Xi^-} > 1$ cm and that of the Λ^0 candidate to be between 2.5 and 50 cm. To enhance the selection of Λ^0 from Ξ^- decays, we require the difference between the Ξ^- and Λ^0 decay lengths to be greater than 1 cm. Finally, it is required that the d_0 of the Ξ^- candidate be less than 0.25 cm and the distance δZ_0 along the z-axis between the Ξ^- and the primary vertex be less than 2 cm.

The invariant mass $M_{\Lambda^0\pi}$ is calculated by fixing the mass of the Λ^0 candidate to 1.1157 GeV/c^2 [19] and assigning the pion mass to the third track. Figure 1 shows the invariant mass for Ξ^- candidates with $|\eta| < 1$ overlaid with the fitted curve.

As for the Λ^0 case, the Ξ^- candidates are divided into 17 p_T intervals and the number of Ξ^- in each interval is determined by fitting the corresponding $M_{\Lambda^0\pi}$ invariant mass distribution using a Gaussian function for the signal and a third-order polynomial for the background. The fitted background is then subtracted bin-by-bin from the data entries in the signal region (1.31 to 1.33 GeV/c^2) to obtain the Ξ^- yield in every p_T interval. The systematic uncertainty of the fit procedure is estimated the same way as for the Λ^0 and is found to change by no more than $\pm 5\%$ in all p_T intervals.

To reconstruct Ω^- decays we follow the same procedure as for the Ξ^- and apply the same selection criteria except that the third track is assigned the kaon mass. The search decay mode is $\Omega^- \rightarrow \Lambda^0 K^- \rightarrow (p\pi^-)K^-$. Because of the larger background, the procedure to extract the Ω^- signal yield is slightly different from that in the previous cases. Track pairs with $M_{p\pi^-}$ in the mass ranges $1.095 - 1.105$ and $1.127 - 1.137$ GeV/c^2 are combined with the third track to obtain the invariant mass distribution of the combinatorial background. This distribution is subtracted from the $M_{\Lambda^0 K^-}$ distribution after normalizing to the number of events in the mass window $1.69 < M_{\Lambda^0 K^-} < 1.74$ GeV/c^2. The background subtracted $M_{\Lambda^0 K^-}$ invariant mass distribution is shown in Figure 1.

The distribution is divided into 10 p_T intervals, and we use the method described above to extract the Ω^- signal from the corresponding invariant mass distributions in each p_T interval within the mass window 1.66 to 1.68 GeV/c^2. The systematic uncertainty due to the fitting procedure is also calculated in a similar manner as Ξ^-, with the exception of using a double Gaussian variation because of low Ω^- statistics. The overall uncertainties are about $\pm 10\%$ for all p_T intervals. The p_T resolution of Ξ^- and Ω^- as a function of p_T is similar to Λ^0.

IV. ACCEPTANCE CALCULATION AND SYSTEMATIC UNCERTAINTIES

The geometric and kinematic acceptance is estimated with Monte Carlo (MC) simulations. The MC data of a resonance state are generated with fixed p_T corresponding to 14 points [18] ranging from 0.75 to 10 GeV/c and flat in rapidity $|y| < 2$. A generated resonance is combined with either one or four non-diffractive inelastic MB events generated with the PYTHIA [20] generator. Although the average number of interactions in our data sample is a little less than two, the default acceptance is calculated from the MC sample with four MB events and the difference of the acceptance values between the two samples is one of our systematics. This is because PYTHIA underestimates the average event multiplicity and based on a study with tracks from K^0_S decay, the sample with four MB events reproduces the low p_T tracking efficiency in data well within the systematic uncertainty.

The detector response to particles produced in the simulation is modeled with the CDF II detector simulation that in turn is based on the GEANT-3 MC program [21]. Simulated events are processed and selected with the same analysis code used for the data. The acceptance is defined as the ratio of the number of reconstructed resonances with the input p_T over the generated number, including the branching ratio. Acceptance values are calculated separately for the particles and their corresponding antiparticles and the average of the two is used as the default value, since the acceptances for the two states are similar. Figure 2 shows the acceptance for the three particles including the branching ratio.

The acceptance values obtained for the 14 p_T points are fitted with a fourth order polynomial function and the fitted curve is used to correct the numbers of each hyperon state in the data as a function of p_T. The modeling of the MB events overlapping with the examined resonance and the selection criteria applied contribute as a systematic uncertainty to the acceptance calculation. The contribution from the former has already been mentioned. Acceptance uncertainties due to the selection criteria are studied by changing the selection values of the variables used to reconstruct the resonances. The variables examined are p_T, $|Z_1 - Z_2|$, $|Z_3 - Z_4|$, δZ_0, d_0 and the decay lengths. For each variable other than p_T, two values around the default value are typically chosen. One value is such that it has little effect on the signal, and the other reduces the signal by $\sim$20 to 30%. The default minimum p_T selection value is 0.325 GeV/c, and it is changed to 0.3 GeV/c and to 0.35 GeV/c.

For each considered variation, a new acceptance curve

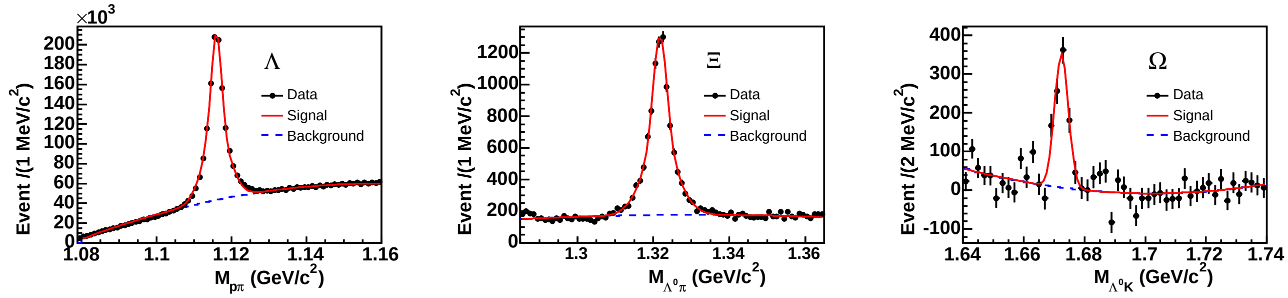

FIG. 1: Reconstructed invariant mass distributions for $M_{p\pi}$ (left), $M_{\Lambda^0\pi}$ (center), and M_{Λ^0K} (right). The background has been subtracted from the M_{Λ^0K} distribution. The solid lines are fitted curves, a third-degree polynomial for the background and either a double ($M_{p\pi}$ and $M_{\Lambda^0\pi}$) or single (M_{Λ^0K}) Gaussian function to model the peak. The widths reflect the tracking resolution and are consistent with the widths from MC simulation.

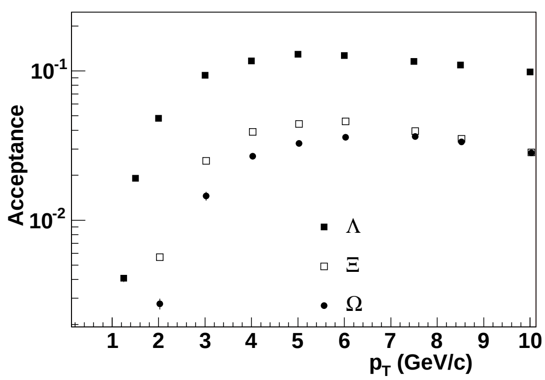

FIG. 2: Acceptances for the three particles, Λ^0, and Ξ^- and Ω^-. The values include the branching ratio to our final states and are averaged acceptances of particles and corresponding antiparticles.

and the number of resonances as a function of p_T are obtained, and the percentage change between the new p_T distribution and the one with the default selection requirements is taken as the uncertainty in the acceptance for the specific p_T interval. The square root of the quadratic sum of the uncertainties from each variation is taken as the total conservative uncertainty on the acceptance in a given p_T bin. The systematic uncertainty associated with the Ω^- hyperon acceptance is derived from the Ξ^- uncertainty estimate since the reconstruction follows the same criteria. This acceptance uncertainty is added quadratically to the systematic uncertainty due to the fitting procedure, described earlier, to give the total systematic uncertainty.

For the Λ^0 case, the acceptance uncertainty decreases from about 25% at $p_T \sim 1$ GeV/c to 10% at $p_T \sim 2$ GeV/c and then rises again slowly to 15% for $p_T > 7$ GeV/c. The corresponding acceptance uncertainty for the Ξ^- (Ω^-) case decreases from about 15% (20%) at $p_T \sim 2$ GeV/c to 10% (15%) for $p_T > 4$ GeV/c.

V. INVARIANT DIFFERENTIAL CROSS SECTION

The inclusive invariant p_T differential cross section for each hyperon resonance is calculated as $Ed^3\sigma/dp^3 = (\sigma_{mb}/N_{event})d^3N/Ap_Tdp_Tdyd\phi = (\sigma_{mb}/2\pi N_{event})\Delta N/Ap_T\Delta p_T\Delta y$ where σ_{mb} is our MB trigger cross section, N_{event} is the number of weighted events, ΔN is the number of hyperons observed in each p_T interval (Δp_T) after background subtraction, A is the acceptance in the specific p_T interval, and Δy is the rapidity range used in the acceptance calculation (-2 to 2).

Figure 3 shows the results for the p_T differential cross section for the three hyperon resonances. The uncertainties shown for each data point include the statistical and all systematic uncertainties described above, except the one associated with σ_{mb} [22]. The cross sections are listed in Table I. The p_T values are the weighted averages within the p_T intervals calculated according to the cross section as a function of p_T , which is obtained from the fit parameters described below.

The p_T differential cross section is modeled by a power law function, $A(p_0)^n/(p_T+p_0)^n$, for $p_T > 2$ GeV/c. In order to compare with the previous CDF K^0_S result [5, 24], p_0 is fixed at 1.3 GeV/c, and the results are shown in Table II. The data $p_T \sim <2$ GeV/c cannot be described well by the power law function even if p_0 is allowed to float. For this region, the data are better described by an exponential function, $Bexp[-b \cdot p_T]$. The results of this fit are shown in Table III, and the slope b of Λ is consistent with previous measurements [11, 12]. The b values depend on the range of the fit but are about two, which corresponds to an average p_T of 1 GeV/c under the assumption that the fit can be extrapolated down to $p_T = 0$ GeV/c.

The bottom plot in Figure 3 shows the ratio of the p_T differential cross sections for Ξ^- and Λ^0, and Ω^- and Λ^0. For the ratio plots, Λ^0 cross sections are recalculated at the Ξ^- and Ω^- p_T values. In the Ξ^-/Λ^0 ratio there is a rise at low p_T, and the ratio reaches a plateau at $p_T > 4$ GeV/c. It should be noted that the Λ^0 cross section also

TABLE I: The values of inclusive invariant p_T differential cross sections ($Ed^3\sigma/dp^3$) in Figure 3. The uncertainties include both statistical and systematic uncertainties.

p_T (GeV/c)	Λ^0 (mb/GeV$^2c^3$)	$p_T(GeV/c)$	$\Xi^\pm$ (mb/GeV$^2c^3$)	$p_T(GeV/c)$	$\Omega^\pm$ (mb/GeV$^2c^3$)
1.24	4.15x10^{-1}± 1.07x10^{-1}	2.11	4.96x10^{-3}± 1.25x10^{-3}	1.96	1.19x10^{-3}± 2.92x10^{-4}
1.34	2.55x10^{-1}± 6.36x10^{-2}	2.36	2.76x10^{-3}± 6.41x10^{-4}	2.46	2.88x10^{-4}± 5.68x10^{-5}
1.44	1.95x10^{-1}± 4.69x10^{-2}	2.61	1.64x10^{-3}± 3.32x10^{-4}	2.96	9.89x10^{-5}± 1.85x10^{-5}
1.54	1.72x10^{-1}± 3.97x10^{-2}	2.86	1.03x10^{-3}± 1.89x10^{-4}	3.43	7.54x10^{-5}± 1.34x10^{-5}
1.69	1.11x10^{-1}± 2.44x10^{-2}	3.11	7.26x10^{-4}± 1.12x10^{-4}	3.91	2.07x10^{-5}± 4.37x10^{-6}
1.89	6.54x10^{-2}± 1.33x10^{-2}	3.36	4.46x10^{-4}± 6.94x10^{-5}	4.47	6.77x10^{-6}± 2.10x10^{-6}
2.09	4.03x10^{-2}± 7.67x10^{-3}	3.61	2.96x10^{-4}± 4.65x10^{-5}	4.97	9.41x10^{-6}± 2.33x10^{-6}
2.29	2.54x10^{-2}± 4.52x10^{-3}	3.86	2.10x10^{-4}± 3.34x10^{-5}	5.63	1.87x10^{-6}± 6.51x10^{-7}
2.49	1.63x10^{-2}± 2.73x10^{-3}	4.11	1.30x10^{-4}± 2.13x10^{-5}	6.84	5.21x10^{-7}± 2.14x10^{-7}
2.69	1.06x10^{-2}± 1.67x10^{-3}	4.36	7.66x10^{-5}± 1.28x10^{-5}	8.78	1.32x10^{-7}± 9.71x10^{-8}
2.89	6.96x10^{-3}± 1.04x10^{-3}	4.61	6.55x10^{-5}± 1.10x10^{-5}		
3.13	4.26x10^{-3}± 6.09x10^{-4}	4.97	3.52x10^{-5}± 5.78x10^{-6}		
3.43	2.30x10^{-3}± 3.16x10^{-4}	5.47	1.81x10^{-5}± 3.20x10^{-6}		
3.78	1.20x10^{-3}± 1.62x10^{-4}	5.98	8.71x10^{-6}± 1.94x10^{-6}		
4.22	5.42x10^{-4}± 7.44x10^{-5}	6.67	3.53x10^{-6}± 8.94x10^{-7}		
4.72	2.42x10^{-4}± 3.63x10^{-5}	7.68	9.02x10^{-7}± 2.77x10^{-7}		
5.22	1.20x10^{-4}± 1.37x10^{-5}	8.95	5.09x10^{-7}± 2.09x10^{-7}		
5.72	6.21x10^{-5}± 7.68x10^{-6}				
6.23	3.38x10^{-5}± 4.76x10^{-6}				
6.73	1.76x10^{-5}± 3.03x10^{-6}				
7.43	8.87x10^{-6}± 1.46x10^{-6}				
8.44	4.10x10^{-6}± 8.29x10^{-7}				
9.44	1.42x10^{-6}± 4.21x10^{-7}				

TABLE II: The results of power law function fits to the inclusive invariant p_T differential cross sections described in the text and shown in Figure 3 for $p_T > 2$ GeV/c. The parameter p_0 is fixed to 1.3 GeV/c in all fits. The values for all charge and K^0_S at $\sqrt{s} = 1.8$ TeV. The uncertainties shown do not include the MB cross section uncertainty [22]. The last line of the table gives the χ^2 per degree-of-freedom of the fit to data.

Parameter (units)	All charged [25]	K^0_S [24]	Λ^0	$\Xi^\pm$	$\Omega^\pm$
A (mb/GeV$^2c^3$)	450 ± 10	45 ± 9	210 ± 25	14.9 ± 2.5	1.50 ± 0.75
p_0 (GeV/c)	1.3	1.3	1.3	1.3	1.3
n	8.28 ± 0.02	7.7 ± 0.2	8.81 ± 0.08	8.26 ± 0.12	8.06 ± 0.34
χ^2/dof	103/65	8.1/11	5.7/15	15.8/15	10.5/7

includes Λ^0 production from the decay of other hyperon states ($\Sigma^0 \rightarrow \Lambda^0\gamma$, $\Xi^\pm$, Ξ^0 and $\overline{\Xi}^0$). Due to the short Σ^0 lifetime, Λ^0 from Σ^0 decays cannot be separated from direct Λ^0 production. Simulations of cascade decays indicate that $\sim 50\%$ of Λ^0 from Ξ decays will satisfy our Λ^0 selection criteria, with the fraction of Λ^0 fairly independent of Ξ p_T. The ratio plots in Figure 3 are fitted to a constant, and the value 0.17 ± 0.01 is obtained for Ξ^-/Λ^0 and 0.025 ± 0.002 for Ω^-/Λ^0.

The ratio and p_T plots in Figure 3 clearly show that the cross sections depend on the number of strange quarks. However, the plots in Figure 3, n values in Table II including K^0_S [24] and all charged particles [25] indicate that the p_T slopes are similar in the high p_T region. This could be an indication of a universality in particle production as p_T increases [26]. This is in contrast to the low p_T region where the slope exhibits a strong particle type dependence [27].

Figure 4 shows the p_T differential cross sections for two charged-particle multiplicity regions, $N_{ch} < 10$ and $N_{ch} > 24$. $N_{ch} = 24$ (10) corresponds to $dN/d\eta \sim 16(7)$, corrected for the track reconstruction efficiency and unreconstructed tracks with $p_T < 0.3$ GeV/c [25]. Due to the low Ω^- sample statistics, distributions are only shown for Λ^0 and Ξ^-. We observe a correlation between high p_T particles and high multiplicity events. This is a general characteristic independent of the particle types. Table IV lists the cross section values in Figure 4.

VI. SUMMARY

The production properties of Λ^0, Ξ^-, and Ω^- hyperons reconstructed from minimum-bias events at $\sqrt{s} = 1.96$ TeV are studied. The inclusive invariant p_T differential

TABLE III: The results of exponential function fits to the inclusive invariant p_T differential cross sections shown in Figure 3 for the p_T ranges given in the second row. The uncertainties shown do not include the MB cross section uncertainty [22]. The last line of the table gives the χ^2 per degree-of-freedom of the fit to data.

Parameter (units)	Λ^0	Λ^0	$\Xi^\pm$	$\Omega^\pm$
p_T range (GeV/c)	[1.2, 2.5]	[1.2, 4]	[1.5, 4]	[2, 4]
B (mb/GeV$^2c^3$)	4.68 ± 1.04	3.16 ± 0.35	0.16 ± 0.04	0.024 ± 0.011
b (GeV^{-1}c)	2.30 ± 0.12	2.10 ± 0.04	1.75 ± 0.08	1.80 ± 0.19
χ^2/dof	1.0/7	7.2/12	4.0/8	6.3/3

TABLE IV: The values of inclusive invariant p_T differential cross sections ($Ed^3\sigma/dp^3$) in Figure 4 for two multiplicity ranges. The uncertainties include both statistical and systematic uncertainties.

p_T (GeV/c)	Λ^0 (mb/GeV$^2c^3$)		p_T (GeV/c)	$\Xi^\pm$ (mb/GeV$^2c^3$)	
	N_{ch} <10	N_{ch} >24		N_{ch} <10	N_{ch} >24
1.24	$1.35\times10^{-1}\pm 3.30\times10^{-2}$	$2.79\times10^{-2}\pm 7.43\times10^{-3}$	2.11	$1.69\times10^{-3}\pm 3.29\times10^{-4}$	$4.41\times10^{-4}\pm 8.65\times10^{-5}$
1.34	$8.93\times10^{-2}\pm 2.10\times10^{-2}$	$1.84\times10^{-2}\pm 4.51\times10^{-3}$	2.36	$1.07\times10^{-3}\pm 1.87\times10^{-4}$	$2.58\times10^{-4}\pm 4.60\times10^{-5}$
1.44	$6.93\times10^{-2}\pm 1.57\times10^{-2}$	$1.33\times10^{-2}\pm 3.14\times10^{-3}$	2.61	$5.61\times10^{-4}\pm 8.91\times10^{-5}$	$1.86\times10^{-4}\pm 2.90\times10^{-5}$
1.54	$5.88\times10^{-2}\pm 1.30\times10^{-2}$	$1.40\times10^{-2}\pm 3.17\times10^{-3}$	2.86	$3.62\times10^{-4}\pm 5.75\times10^{-5}$	$1.23\times10^{-4}\pm 1.96\times10^{-5}$
1.69	$3.91\times10^{-2}\pm 8.28\times10^{-3}$	$1.02\times10^{-2}\pm 2.18\times10^{-3}$	3.11	$2.68\times10^{-4}\pm 4.27\times10^{-5}$	$1.03\times10^{-4}\pm 1.61\times10^{-5}$
1.90	$2.34\times10^{-2}\pm 4.72\times10^{-3}$	$6.64\times10^{-3}\pm 1.35\times10^{-3}$	3.36	$1.56\times10^{-4}\pm 2.62\times10^{-5}$	$6.07\times10^{-5}\pm 9.90\times10^{-6}$
2.09	$1.44\times10^{-2}\pm 2.77\times10^{-3}$	$4.53\times10^{-3}\pm 8.82\times10^{-4}$	3.61	$1.03\times10^{-4}\pm 1.84\times10^{-5}$	$4.33\times10^{-5}\pm 7.23\times10^{-6}$
2.29	$8.95\times10^{-3}\pm 1.66\times10^{-3}$	$3.10\times10^{-3}\pm 5.83\times10^{-4}$	3.86	$7.52\times10^{-5}\pm 1.37\times10^{-5}$	$3.06\times10^{-5}\pm 5.42\times10^{-6}$
2.50	$5.59\times10^{-3}\pm 1.01\times10^{-3}$	$2.12\times10^{-3}\pm 3.87\times10^{-4}$	4.12	$5.07\times10^{-5}\pm 1.05\times10^{-5}$	$1.87\times10^{-5}\pm 3.61\times10^{-6}$
2.69	$3.64\times10^{-3}\pm 6.38\times10^{-4}$	$1.46\times10^{-3}\pm 2.60\times10^{-4}$	4.42	$1.90\times10^{-5}\pm 5.18\times10^{-6}$	$1.21\times10^{-5}\pm 2.53\times10^{-6}$
2.90	$2.39\times10^{-3}\pm 4.11\times10^{-4}$	$9.85\times10^{-4}\pm 1.73\times10^{-4}$	4.79	$1.72\times10^{-5}\pm 3.79\times10^{-6}$	$7.48\times10^{-6}\pm 1.68\times10^{-6}$
3.13	$1.43\times10^{-3}\pm 2.41\times10^{-4}$	$6.35\times10^{-4}\pm 1.09\times10^{-4}$	5.33	$8.59\times10^{-6}\pm 1.81\times10^{-6}$	$3.74\times10^{-6}\pm 7.71\times10^{-7}$
3.44	$8.06\times10^{-4}\pm 1.34\times10^{-4}$	$3.61\times10^{-4}\pm 6.19\times10^{-5}$	6.87	$8.22\times10^{-7}\pm 3.80\times10^{-7}$	$3.61\times10^{-7}\pm 9.16\times10^{-8}$
3.79	$4.09\times10^{-4}\pm 6.81\times10^{-5}$	$2.03\times10^{-4}\pm 3.48\times10^{-5}$			
4.22	$1.74\times10^{-4}\pm 2.96\times10^{-5}$	$1.02\times10^{-4}\pm 1.78\times10^{-5}$			
4.72	$7.44\times10^{-5}\pm 1.34\times10^{-5}$	$4.80\times10^{-5}\pm 9.02\times10^{-6}$			
5.22	$3.74\times10^{-5}\pm 6.88\times10^{-6}$	$2.47\times10^{-5}\pm 5.04\times10^{-6}$			
5.72	$1.93\times10^{-5}\pm 3.90\times10^{-6}$	$1.27\times10^{-5}\pm 2.90\times10^{-6}$			
6.42	$6.81\times10^{-6}\pm 1.52\times10^{-6}$	$5.36\times10^{-6}\pm 1.28\times10^{-6}$			
8.00	$1.44\times10^{-6}\pm 3.69\times10^{-7}$	$1.11\times10^{-6}\pm 3.37\times10^{-7}$			

cross sections are well modeled by a power law function above 2 GeV/c p_T. With fixed p_0, the fit parameter n decreases from 8.81 ± 0.08 (Λ^0) to 8.06 ± 0.34 (Ω^-). The low p_T regions are modeled by an exponential function. The exponential slope, b, decreases by $\sim$ 15% from Λ^0 to Ω^-. The cross section ratios Ξ^-/Λ^0 and Ω^-/Λ^0 are presented as a function of p_T. Although the ratios exhibit a strong dependence on the number of strange quarks, the n values of the hyperons, K^0_S and all charged particles are within $\sim$ 10% of each other. This could be an evidence that these particles are produced similarly in p_T as p_T increases regardless of the number of quarks and quark flavors in particles. We also find the hyperon inclusive invariant p_T distributions fall off faster with p_T for low multiplicity events than for high multiplicity events.

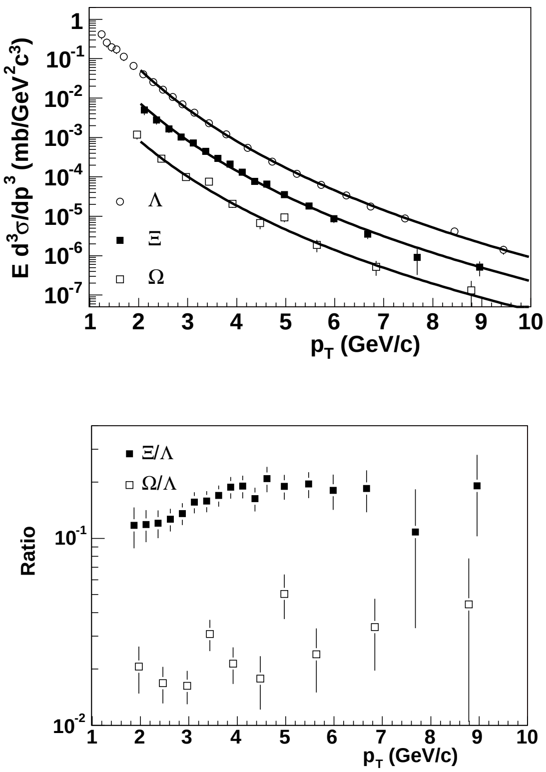

FIG. 3: The inclusive invariant p_T differential cross section distributions for Λ^0, Ξ^-, and Ω^- within $|\eta| < 1$ (top). The solid curves are from fits to a power law function, with the fitted parameters given in Table II. The ratios of Ξ^-/Λ^0 and Ω^-/Λ^0 as a function of p_T (bottom).

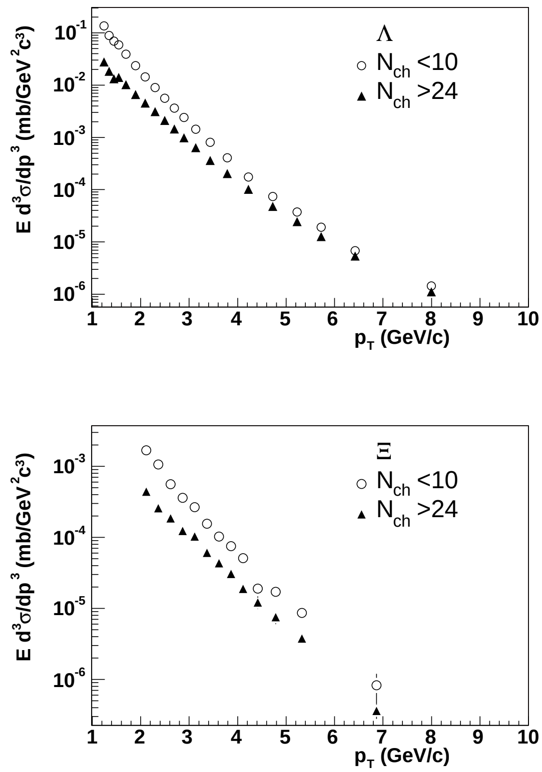

FIG. 4: Inclusive p_T distributions for two charged-particle multiplicity regions, $N_{ch} < 10$ and $N_{ch} > 24$. Distributions for Λ^0 are shown on the top while distributions for Ξ^- are shown on the bottom.

We thank the Fermilab staff and the technical staffs of the participating institutions for their vital contributions. This work was supported by the U.S. Department of Energy and National Science Foundation; the Italian Istituto Nazionale di Fisica Nucleare; the Ministry of Education, Culture, Sports, Science and Technology of Japan; the Natural Sciences and Engineering Research Council of Canada; the National Science Council of the Republic of China; the Swiss National Science Foundation; the A.P. Sloan Foundation; the Bundesministerium für Bildung und Forschung, Germany; the World Class University Program, the National Research Foundation of Korea; the Science and Technology Facilities Council and the Royal Society, UK; the Institut National de Physique Nucleaire et Physique des Particules/CNRS; the Russian Foundation for Basic Research; the Ministerio de Ciencia e Innovación, and Programa Consolider-Ingenio 2010, Spain; the Slovak R&D Agency; and the Academy of Finland.

---

[1] G. D. Rochester and C. C. Butler, Nature **160**, 855 (1947).

[2] M. Athoff *et al.* (TASSO Collaboration), Z. Phys. **C 27**, 27 (1985); W. Braunschweig *et al.* (TASSO Collaboration), Z. Phys. **C 47**, 167 (1990); H. Aihara *et al.* (TPC Collaboration), Phys. Rev. Lett. **54**, 274 (1985); D. De La Vaissiere *et al.* (MARK-II Collaboration), Phys. Rev. Lett. **54**, 2071 (1985); H. Schellman *et al.* (MARK-II Collaboration), Phys. Rev. **D 31**, 3013 (1985); M. Derrick *et al.* (HRS Collaboration), Phys. Rev. **D 35**, 2639 (1987); W. Braunschweig *et al.* (TASSO Collaboration), Z. Phys. **C 45**, 209 (1989); H. Behrend *et al.* (CELLO Collaboration), Z. Phys. **C 46**, 397 (1990); D. Buskulic *et al.* (ALEPH Collaboration), Z. Phys. **C 64**, 361 (1994); P. Abreu *et al.* (DELPHI Collaboration), Z. Phys. **C 65**, 587 (1995); M. Acciarri *et al.* (L3 Collaboration), Phys. Lett. **B 328**, 223 (1994); P. Acton *et al.* (OPAL Collaboration), Phys. Lett. **B 291**, 503 (1992).

[3] M. Derrick *et al.* (ZEUS Collaboration), Z. Phys. **C 68**, 29 (1995); J. Breitweg *et al.*, Eur. Phys. J. **C 2**, 77, (1998); S. Akid *et al.* (H1 Collaboration), Nucl. Phys. **B 480**, 3 (1996); C. Adloff *et al.* (H1 Collaboration), Z. Phys. **C 76**, 213 (1997).

[4] R. Ansoge *et al.* (UA5 Collaboration), Z. Phys. **C 41**, 179 (1988); R. Ansoge *et al.* (UA5 Collaboration), Nucl. Phys. **B 328**, 36 (1989); G. Bocquet *et al.* (UA1 Collaboration), Phys. Lett. **B 366**, 441 (1996).

[5] D. Acosta *et al.* (CDF Collaboration), Phys. Rev. **D 72**, 052001 (2005).

[6] B. I. Abelev *et al.* (STAR Collaboration), Phys. Rev. **C 75**, 064901, (2007).

[7] P. Koch, B. Mueller and J. Rafelski, Phys. Rep. **142**, 321 (1986).

[8] M. Bourquin *et al.* (Bristol-Geneva-Heidelberg-Orsay-Rutherford-Strasbourg Collaboration), Z. Phys. C **5**, 275 (1980).

[9] T. Akesson *et al.* (Axial Field Spectrometer Collaboration), Nucl. Phys. B **246**, 1 (1984).

[10] G. J. Alner *et al.* (UA5 Collaboration), Phys. Lett. B **151**, 309 (1985).

[11] S. Banerjee *et al.* (E735 Collaboration), Phys. Rev. Lett. **62**, 12 (1989).

[12] T. Alexopoulos *et al.* (E735 Collaboration), Phys. Rev. D **46**, 2773 (1992).

[13] A. Abulencia *et al.* (CDF Collaboration), J. Phys. G **34**, 2457 (2007).

[14] A. Sill *et al.*, Nucl. Instrum. Methods A **447**, 1 (2000).

[15] In the CDF coordinate system, θ and ϕ are the polar and azimuthal angles of a track, respectively, defined with respect to the proton beam direction, z. The pseudo-rapidity η is defined as $-\ln[\tan(\theta/2)]$. The transverse-momentum of a particle is $p_T = p\sin\theta$. The rapidity is defined as $y = 0.5\ln[(E+p_z)/(E-p_z)]$, where E and p_z are the energy and longitudinal momentum of the particles associated with the track.

[16] A. Affolder *et al.* (CDF Collaboration), Nucl. Instrum. Methods A **526**, 249 (2004).

[17] D. Acosta *et al.*, Nucl. Instrum. Methods A **494**, 57 (2002).

[18] The number of p_T intervals for data is dictated by statistics such that the fits to the invariant mass distributions are stable. In the acceptance calculation, the number of p_T points is chosen such that a smooth acceptance curve as a function of p_T can be obtained. The statistical uncertainties of acceptance values are less than a few percent.

[19] C. Amsler *et al.* (Particle Data Group), Phys. Lett. B **667**, 1 (2008).

[20] T. Sjöstrand, P. Eden, C. Friberg, L. Lonnblad, G. Miu, S. Mrenna, and E. Norrbin, Comput. Phys. Commun. **135**, 238 (2001). The version used in this paper is 6.327.

[21] R. Brun, R. Hagelberg, M. Hansroul, and J. C. Lassalle, version 3.15, CERN-DD-78-2-REV.

[22] The total cross section corresponding to the minimum-bias trigger is estimated to be 45 ± 8 mb. The elastic (17 ± 4 mb [19]), single diffractive SD (12 mb), and half of the double diffractive DD (4 mb) cross sections are subtracted from the total $p\overline{p}$ cross section ($78{\pm}6$ mb [19] [23]) to give this estimate. The SD and DD cross sections are estimated using PYTHIA [20], and no uncertainties are assigned to SD and DD cross section. A simulation study shows that the minimum-bias trigger is sensitive to $\sim 100\%$ of inelastic events which are not SD or DD and $\sim 50\%$ of DD events. A 100% uncertainty is assigned to the DD contribution attributing to the uncertainty in the event characteristics and detector simulation.

[23] J.R. Cudell *et al.* (COMPETE Collaboration), arXiv:hep-ph/0206172V1.

[24] F. Abe *et al.* (CDF Collaboration), Phys. Rev. D **40**, 3791 (1989).

[25] F. Abe *et al.* (CDF Collaboration), Phys. Rev. Lett. **16**, 1819 (1988). This is at $\sqrt{s} = 1800$ GeV

[26] A manuscript on a high statistics measurement of $K^0_S, K^{*\pm}(892)$ and $\phi^0(1020)$ production properties is in preparation.

[27] A.M. Rossi *et al.*, Nucl. Phys. **B 84**, 269 (1975); R.E. Ansorge *et al.* (UA5 Collaboration), Phys. Lett. B **199**, 311 (1987); G.J. Alner *et al.* (UA5 Collaboration), Nucl. Phys. **B 258**, 505 (1985); S. Banerjee *et al.* (E735 Col-

laboration), Phys. Rev. Lett. **64**, 991 (1990).